

Feasibility of Lead and Tungsten GRID Collimators for Electron GRID Therapy

Melody Liu, ZhengZheng Xu, Hualin Zhang, Brittney Chau, Lauren Garcia, Lauren Lukas

Department of Radiation Oncology, Norris Comprehensive Cancer Center, University of Southern California

USC University of Southern California

Abstract

Objectives: Photon based spatially fractionated radiation therapy (SFRT) has been shown to have immunomodulatory effects on the tumor microenvironment¹. There is a need to develop SFRT strategies using electrons for cutaneous tumors for which the tumor microenvironment is involved in disease progression and immune evasion, such as mycosis fungoides. Lead collimator field-shaping is widely used in radiation oncology for electron beam radiation therapy for treatment of superficial and skin malignancies, including mycosis fungoides. Currently there are no clinical studies of electron SFRT (eSFRT) or evaluation of the immunomodulatory effects of eSFRT in mycosis fungoides. The purpose of this study is to assess the feasibility and dosimetry of GRID collimators designed for eSFRT delivery using lead and tungsten filament.

Methods: GRID collimators were designed with lead (1.5 mm and 3.0 mm thick) and tungsten filament (1.0 mm thick) sheets, featuring a hexagonal pattern of 27 holes (1.5 cm diameter, 2.0 cm spacing). Percent depth doses (PDD) and cross beam plane dose profiles for 6, 9, and 12 MeV electron beams on TrueBeam STX were measured using a water tank scanning system. The 10 x 10 cm² cone was mounted, the water surface set at 100 cm, and the GRID collimator placed directly onto the cone cut-out position. Depths of maximum (dmax), 90% (d90), and 50% (d50) doses were determined from the PDD curve, and peak to valley dose ratios (PVDR) were evaluated at various depths.

Results: PDDs for 6, 9, and 12 MeV electron beams with lead and tungsten filament GRID collimators were measured. For 6 MeV: dmax was 8.4, 8.0, and 8.0 mm; d90 was 13.3, 13.4, and 12.7 mm; and d50 was 20.7, 20.7, and 20.3 mm. For 9 MeV: dmax was 8.3, 9.5, and 8.3 mm; d90 was 15.9, 16.3, and 17.5 mm; and d50 was 28.0, 29.3, and 29.5 mm. For 12 MeV: dmax was 10.7, 6.7, and 15.6 mm; d90 was 19.1, 17.7, and 22.9 mm; and d50 was 35.3, 35.3, and 40.3 mm. PVDRs were also measured. For 6 MeV: dmax was 4.25, 5.65, and 2.78 mm; d90 was 2.27, 2.50, and 1.92 mm. For 9 MeV: dmax was 3.28, 5.55, and 2.08 mm; d90 was 2.11, 2.81, and 1.63 mm. For 12 MeV: dmax was 2.54, 5.08, and 2.01 mm; d90 was 2.05, 2.90, and 1.5 mm. Compared to published data using a 1 mm thick tungsten rubber GRID collimator², this study showed more superficial PDD and larger PVDR at dmax and d90 for all lead and tungsten filament GRID collimators.

Conclusions: Lead and tungsten filament GRID collimators can deliver dose distributions suitable for eSFRT. Lead sheets are flexible and can be placed on the skin (with an additional covering) or on the linac electron treatment cone. Tungsten filament, being biocompatible, may be more favorable in clinics, but its cost may limit availability. Further research is needed to evaluate preclinical models of eSFRT for mycosis fungoides to assess tumor microenvironment immune effects.

Introduction

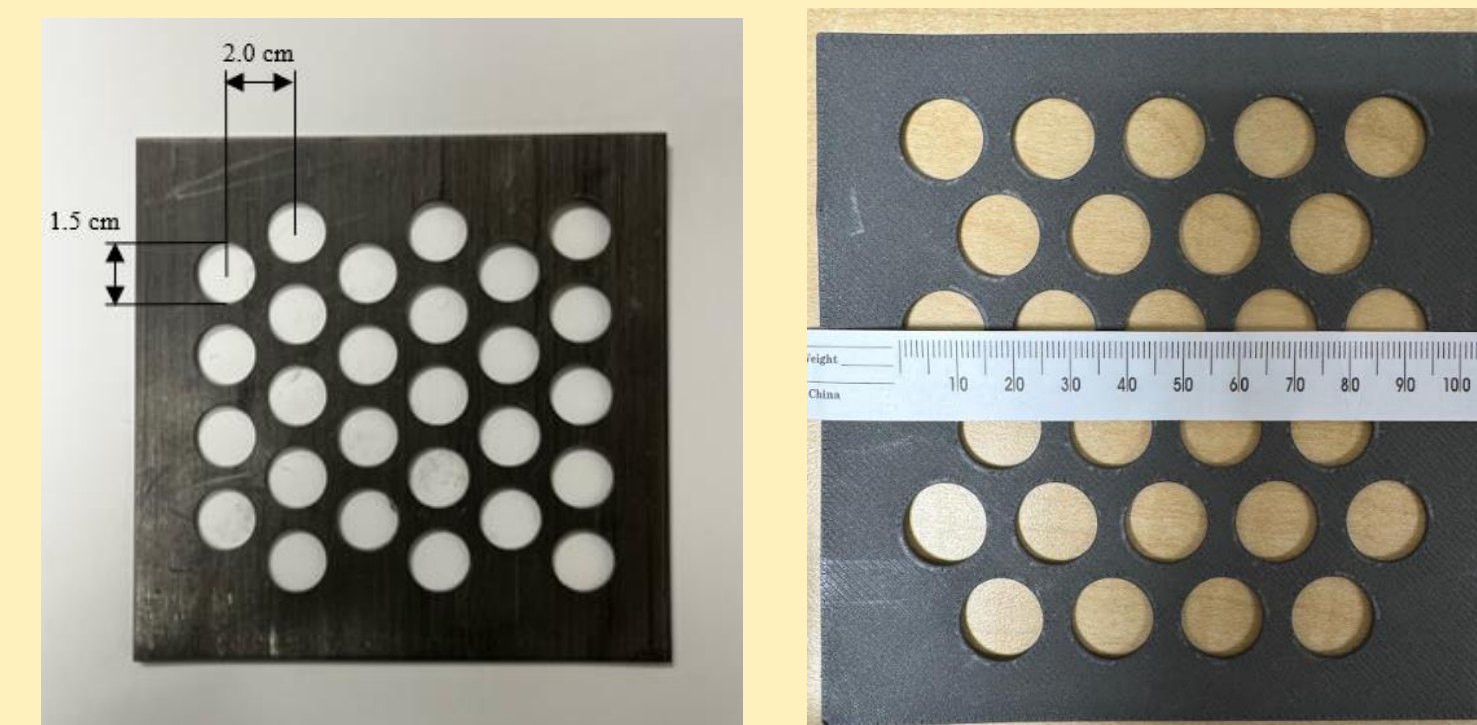
Spatially fractionated radiation therapy (SFRT) delivers a high ablative dose to small tumor volumes while minimizing peripheral doses to surrounding normal tissue. Photon-based SFRT supports bulky tumor control without significantly increasing toxicity and may enhance the immune response within the targeted tumor and nonirradiated tumors³. Electron beam SFRT (eSFRT) has different dosimetric characteristics and may be more effective for superficial and cutaneous tumors due to the sharp dose drop-off beyond the tumor. The immunomodulatory effects of eSFRT could benefit tumors like cutaneous lymphoma, where immunopathogenesis affects prognosis.

Cutaneous T cell lymphoma (CTCL) is a heterogeneous group of non-Hodgkin's lymphomas involving skin-tropic T cell malignancies, with mycosis fungoides (MF) and Sezary syndrome (SS) as classic types. Electron beam therapy, including total skin electron beam therapy, is commonly used for palliative treatment of CTCL. However, the immune effects of eSFRT on CTCL are unknown, necessitating further evaluation. The design of eSFRT collimators must be experimentally determined for each patient to cover the target, including the therapeutic region as determined by the depth-dose profile, and must produce an adequate peak-to-valley dose ratio (PVDR) from the lateral dose profile⁴. The dosimetric characteristics must be verified to determine the output factor and monitor unit (MU) values based on measurements before any clinical use takes place. We present a feasibility assessment of novel lead and tungsten filament (TF) GRID collimators for eSFRT using a phantom study. The dosimetric characteristics and possible clinical applications are presented.

Methodology

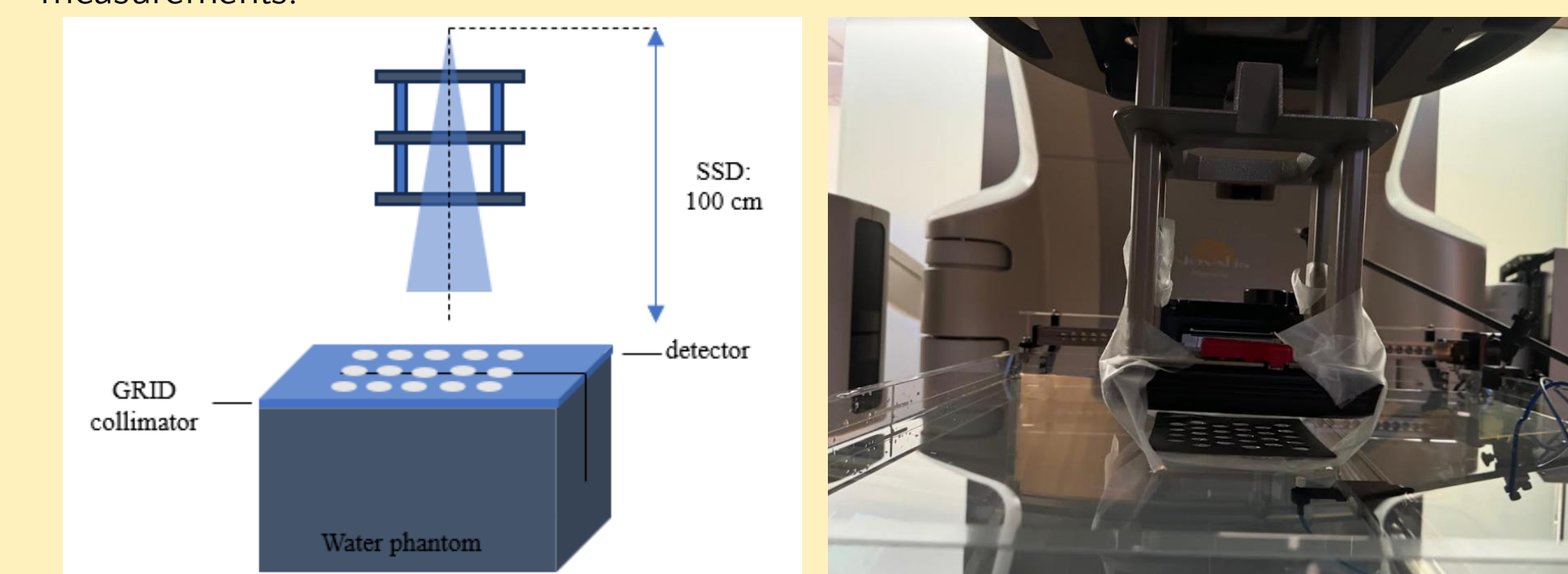
Lead and Tungsten Filament GRID Collimators: The dosimetric characteristics of the lead and TF GRID collimators in eSFRT were evaluated with water tank measurements. The aperture diameter of the holes was 1.5 cm and the center-to-center spacing of the holes was 2.0 cm for a total of 27 holes in 10 x 10 cm² sheets. The schema of the GRID collimators is shown in Figure 1. All GRID collimators were produced by the Dornsife-Viterbi Machine Shop at the University of Southern California. The Lead GRID collimators were created using lead sheets (Radiation Products Design, Albertville, MN, USA) in thicknesses of 1.5 mm and 3.0 mm. The tungsten filament (TF) GRID collimator was created by 3D printing using tungsten filament comprised of tungsten (91.0–93% by weight), a binding additive (proprietary), and poly(lactic acid) (Rapid 3DShield Tungsten Filament[®], Rapid 3DShield, LLC, Stoughton, WI, USA) with physical properties summarized in Table 1. There was no post sintering of the print. The TF GRID collimator was 1.0 mm thick.

Figure 1. Schema of the GRID collimators. The aperture diameter was 1.5 cm and the center-to-center spacing of the holes was 2.0 cm for a total of 27 holes on a 10 x 10 cm² sheet. Left: lead GRID collimator; Right: TF GRID collimator.



Water Tank Measurements: The characterization of the GRID field includes: (1) measuring the percent depth dose (PDD) curves at the central hole; (2) measuring the depths of maximum percent depth dose (dmax); (3) acquiring the inline and crossline dose profiles at different depths; (4) measuring the peak to valley dose ratios (PVDR) at different depths; (5) measuring the output factors at different depths. The PDD of the central hole of the GRID collimator center and the dose profiles were measured with PTW BEAMSCAN system (Freiburg, Germany) and a microdiamond detector (PTW Freiburg, Germany). The geometry for the measurements of the depth and lateral dose profiles with the GRID collimators is shown in Figure 2. Electron beams of nominal energy 6 MeV, 9 MeV, and 12 MeV on a linear accelerator (Truebeam STX, Varian Medical Systems, Palo Alto, CA, USA) with a 10 x 10 cm² electron applicator were used for the dosimetric parameter measurements of the open and GRID fields. The electron beams were then collimated with the lead and TF GRID collimators placed on the surface of a water phantom. The depths of the maximum dose (dmax), 90% dose (d90) and 50% dose (d50) in the virtual water phantom were evaluated from PDD data. Then, the lateral dose profiles were evaluated at dmax and d90 for deriving the peak to valley ratios (PVDR), defined as dose ratios between the open to the blocked area doses. The PVDRs were calculated from the ratios of the average values at the centers of four blocked areas and five open areas.

Figure 2. Diagram of the experimental set up for film dosimetry utilizing a water bath phantom with film placed parallel to the beam's central axis for PDD and lateral dose profile measurements.



Results

The PDDs of the open and GRID collimated electron beams
The tabulated PDDs of the open, 1.5 mm and 3.0 mm lead and 1 mm TF GRID collimated electron beams, respectively, are presented in Table 2.

Table 2. Percentage depth dose data of 10x10cm² open and GRID fields

| depth(mm) | 6 MeV | | | | 9 MeV | | | | 12 MeV | | | |
|-----------|-------|------------------|----------------|--------------|-------|------------------|----------------|--------------|--------|------------------|----------------|--------------|
| | Open | 1.5 mm Lead GRID | 3 mm Lead GRID | 1 mm TF GRID | Open | 1.5 mm Lead GRID | 3 mm Lead GRID | 1 mm TF GRID | Open | 1.5 mm Lead GRID | 3 mm Lead GRID | 1 mm TF GRID |
| 5 | 85.4 | 97.1 | 98.2 | 96.2 | 90.3 | 95.7 | 99.7 | 97.2 | 92.5 | 96.8 | 97.9 | 92.9 |
| 8 | 91.9 | 100.0 | 100.0 | 100.0 | 92.5 | 98.8 | 99.7 | 99.9 | 94.5 | 99.7 | 98.1 | 97.8 |
| 10 | 95.9 | 99.3 | 98.9 | 98.3 | 94.4 | 98.4 | 98.3 | 98.0 | 96.2 | 92.9 | 88.3 | 98.7 |
| 12 | 98.9 | 98.4 | 95.0 | 93.3 | 96.2 | 99.1 | 78.0 | 74.5 | 99.1 | 100.0 | 66.4 | 64.3 |
| 14 | 100.0 | 87.3 | 86.9 | 84.6 | 98.3 | 100.0 | 61.5 | 59.9 | 98.3 | 93.5 | 45.1 | 47.2 |
| 16 | 98.3 | 76.8 | 76.6 | 74.2 | 98.3 | 89.7 | 41.7 | 44.5 | 98.3 | 81.9 | 36.5 | 39.7 |
| 18 | 92.9 | 65.2 | 65.3 | 62.6 | 98.3 | 78.0 | 27.2 | 30.8 | 98.3 | 63.6 | 21.2 | 26.2 |
| 20 | 83.3 | 53.7 | 54.0 | 51.4 | 98.3 | 66.1 | 15.0 | 15.2 | 98.3 | 47.8 | 23.0 | 24.2 |
| 22 | 69.6 | 42.4 | 42.2 | 40.3 | 98.3 | 35.3 | 10.6 | 19.5 | 98.3 | 31.5 | 8.4 | 17.0 |
| 24 | 53.4 | 31.9 | 31.8 | 30.2 | 98.3 | 22.9 | 6.4 | 17.0 | 98.3 | 15.6 | 22.9 | 40.1 |
| 26 | 42.5 | 22.7 | 22.7 | 20.3 | 98.3 | 13.4 | 8.0 | 13.2 | 98.3 | 8.0 | 13.2 | 20.7 |
| 28 | 32.8 | 15.9 | 16.3 | 17.5 | 98.3 | 8.3 | 9.5 | 8.3 | 98.3 | 8.0 | 12.7 | 20.2 |
| 30 | 28.0 | 15.9 | 16.3 | 17.5 | 98.3 | 8.3 | 9.5 | 8.3 | 98.3 | 8.0 | 12.7 | 20.2 |
| 32 | 22.9 | 15.9 | 16.3 | 17.5 | 98.3 | 8.3 | 9.5 | 8.3 | 98.3 | 8.0 | 12.7 | 20.2 |
| 34 | 19.1 | 15.9 | 16.3 | 17.5 | 98.3 | 8.3 | 9.5 | 8.3 | 98.3 | 8.0 | 12.7 | 20.2 |
| 36 | 15.9 | 15.9 | 16.3 | 17.5 | 98.3 | 8.3 | 9.5 | 8.3 | 98.3 | 8.0 | 12.7 | 20.2 |
| 38 | 12.7 | 15.9 | 16.3 | 17.5 | 98.3 | 8.3 | 9.5 | 8.3 | 98.3 | 8.0 | 12.7 | 20.2 |
| 40 | 10.7 | 15.9 | 16.3 | 17.5 | 98.3 | 8.3 | 9.5 | 8.3 | 98.3 | 8.0 | 12.7 | 20.2 |
| 42 | 8.4 | 15.9 | 16.3 | 17.5 | 98.3 | 8.3 | 9.5 | 8.3 | 98.3 | 8.0 | 12.7 | 20.2 |
| 44 | 8.0 | 15.9 | 16.3 | 17.5 | 98.3 | 8.3 | 9.5 | 8.3 | 98.3 | 8.0 | 12.7 | 20.2 |
| 46 | 8.0 | 15.9 | 16.3 | 17.5 | 98.3 | 8.3 | 9.5 | 8.3 | 98.3 | 8.0 | 12.7 | 20.2 |
| 48 | 8.0 | 15.9 | 16.3 | 17.5 | 98.3 | 8.3 | 9.5 | 8.3 | 98.3 | 8.0 | 12.7 | 20.2 |
| 50 | 8.0 | 15.9 | 16.3 | 17.5 | 98.3 | 8.3 | 9.5 | 8.3 | 98.3 | 8.0 | 12.7 | 20.2 |

Measured values of depth of dmax, d90 and d80 from the PDDs for the GRID collimated electron beams with lead and TF GRID collimators are presented in Table 3.

Table 3. Measured values of depth of dmax, d90, and d50 from the PDDs for the GRID collimated 6 MeV, 9 MeV, and 12 MeV electron beams with lead and TF GRID collimators

| Energy (MeV) | GRID Collimator | Depth of GRID electron beams (mm) | | |
|--------------|------------------|-----------------------------------|------|------|
| | | dmax | d90 | d50 |
| 6 | Lead GRID 1.5 mm | 8.4 | 13.3 | 20.6 |
| | Lead GRID 3 mm | 8.0 | 13.2 | 20.7 |
| | TF GRID 1 mm | 8.0 | 12.7 | 20.2 |
| 9 | Lead GRID 1.5 mm | 8.7 | 15.9 | 27.7 |
| | Lead GRID 3 mm | 6.0 | 16.2 | 29.3 |
| | TF GRID 1 mm | 11.6 | 17.7 | 29.5 |
| 12 | Lead GRID 1.5 mm | 10.6 | 19.5 | 35.3 |
| | Lead GRID 3 mm | 6.4 | 17.0 | 36.0 |
| | TF GRID 1 mm | 15.6 | 22.9 | 40.1 |

Beam profiles of GRID collimated beams and PVDR

Cross plane beam profiles for the GRID collimated electron beams at each lead and TF GRID collimator thickness at dmax and d90 are shown in Figure 3. The mean PVDR at dmax and d90 at each lead and TF GRID collimator thickness are shown in Table 4.

Figure 3. Electron beam GRID profiles (at d90) using 1.5mm and 3.0mm thickness lead GRID sheets, and tungsten GRID sheet, respectively.

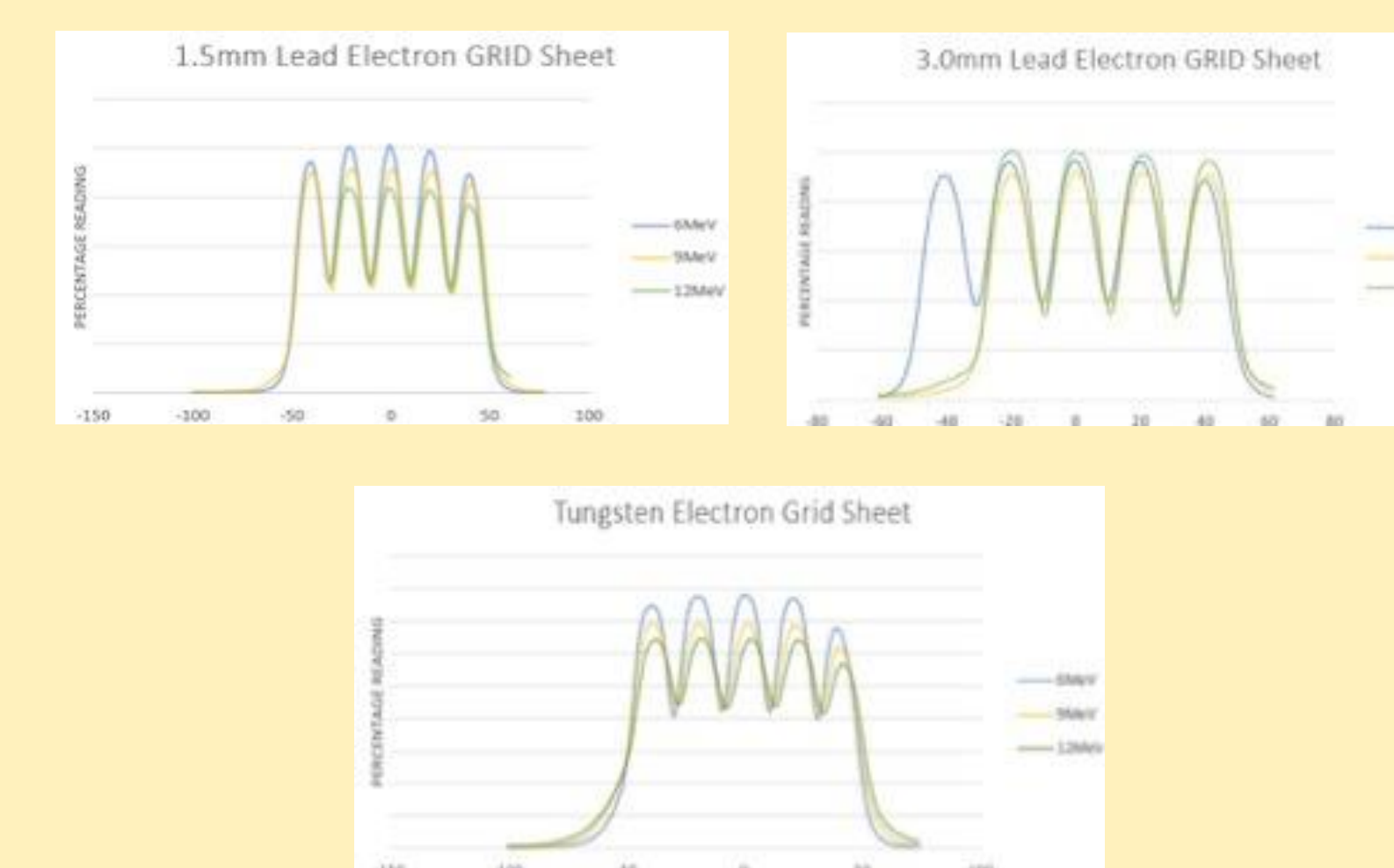


Table 4. Measured PVDR at dmax and d90 for the GRID collimated electron beams

| Energy (MeV) | GRID Collimator | PVDR | |
|--------------|--------------------|------|------|
| | | dmax | d90 |
| 6 | Lead GRID - 1.5 mm | 4.31 | 2.31 |
| | Lead GRID - 3 mm | 5.88 | 2.5 |
| | TF GRID - 1 mm | 2.56 | 1.95 |
| 9 | Lead GRID - 1.5 mm | 3.17 | 2.22 |
| | Lead GRID - 3 mm | 6.96 | 2.47 |
| | TF GRID - 1 mm | 2.04 | 1.65 |
| 12 | Lead GRID - 1.5 mm | 2.51 | 2.01 |
| | Lead GRID - 3 mm | 5.08 | 2.94 |
| | TF GRID - 1 mm | 1.92 | 1.55 |

Discussion

This study evaluated the feasibility and dosimetric characteristics of novel lead and TF GRID collimators for eSFRT using a water bath phantom. Tungsten filament for 3D printing was used to create the TF GRID collimator, which was made to be 1 mm thick and relatively rigid. With moderate bending, the TF GRID collimator may fracture. Lead GRID collimators did not require 3D printing and had better material supply access. Lead sheets can be placed on the skin with an additional covering to protect against lead toxicity. Although more biocompatible, TF can cause potential skin irritation and thus a covering sheet may still be needed.

There were no significant differences in PDDs and PVDRs for lead and TF GRID collimators at 6, 9, and 12 MeV. Both lead and TF GRID collimators achieved a PVDR of ≥ 2 at dmax, although TF GRID collimator PVDRs were less than 2 at d90. Dosimetric parameters for 9 MeV were compared to a published 1 mm thick tungsten rubber GRID collimator², showing a more superficial PDD and larger PVDR at dmax and d90 for lead and TF GRID collimators.

Although eSFRT has not been reported in clinical series, since photon-based SFRT has shown promising results and GRID therapy was initially developed for treating skin cancers, further research of eSFRT could provide insight into the biological mechanisms of eSFRT and leverage its potential to improve response and reduce toxicity from electron treatment. It is speculated that eSFRT could allow sparing of vasculature and immune cells within the treated area, limiting toxicity while contributing to tumor eradication in cutaneous T-cell lymphoma, such as mycosis fungoides.

Conclusions

This study demonstrated that it is feasible for a lead and TF GRID collimators to deliver a dose distribution amenable for eSFRT. Increased thickness of a TF GRID collimator warrants evaluation to achieve a PVDR of ≥ 2 , as the current 1 mm thick TF GRID collimator had a PVDR of less than 2 at d90 for all energies. Lead sheets are flexible and can be placed either on skin (with an additional covering to protect skin) or on to the linac electron treatment cone. An e-GRID made from biocompatible material, such as tungsten filament, may be more favorable in clinic, but may not be readily available in all clinics due to cost. Further research is warranted to evaluate preclinical models of eSFRT for mycosis fungoides to assess tumor microenvironment immune effects.

References

- Lukas L, Zhang H, Cheng K, Epstein A. Immune Priming with Spatially Fractionated Radiation Therapy. *Curr Oncol Rep.* 2023;25(12):1483–95
- Kijima K, Krisanachinda A, Tamura M, Nishimura Y, Monzen H. Feasibility of a Tungsten Rubber Grid Collimator for Electron Grid Therapy. *Anticancer Res.* 2019;39(6):2799–804.
- Iori F, Cappelli A, D'Angelo E, Cozzi S, Chersi SF, De Felice F, Ciammella P, Bruni A, Iotti C. Lattice Radiation Therapy in clinical practice: A systematic review. *Clin Transl Radiat Oncol.* 2023;39:100569.
- Monzen H, Tamura M. Electron Beam SFRT. In: Zhang H, Mayr N, editors. *Spatially Fractionated, Microbeam and FLASH Radiation Therapy* 2023.